Limiting efficiencies of ideal single and multiple energy gap terrestrial solar cells

C. H. Henry
Bell Laboratories, Murray Hill, New Jersey 07974

(Received 14 January 1980; accepted for publication 9 April 1980)

The maximum efficiencies of ideal solar cells are calculated for both single and multiple energy gap cells using a standard air mass 1.5 terrestrial solar spectrum. The calculations of efficiency are made by a simple graphical method, which clearly exhibits the contributions of the various intrinsic losses. The maximum efficiency, at a concentration of 1 sun, is 31%. At a concentration of 1000 suns with the cell at 300 K, the maximum efficiencies are 37, 50, 56, and 72% for cells with 1, 2, 3, and 36 energy gaps, respectively. The value of 72% is less than the limit of 93% imposed by thermodynamics for the conversion of direct solar radiation into work. Ideal multiple energy gap solar cells fall below the thermodynamic limit because of emission of light from the forward-biased *p-n* junctions. The light is radiated at all angles and causes an entropy increase as well as an energy loss.

PACS numbers: 84.60.Jt, 85.30.De

I. INTRODUCTION

The efficiencies of real solar cells have many extrinsic limitations which in principle can be eliminated. These include losses due to reflection, contact shadowing, series resistance, incomplete collection of photogenerated carriers, absorption in inactive window layers, nonradiative recombination, and above ambient cell temperature. Even if these losses are completely eliminated, there remain two *intrinsic* losses which then determine the efficiencies of ideal solar cells. The first are losses because of the inability of a single energy gap solar cell to properly match the broad solar spectrum. Solar photons with energies $\hbar\omega$ less than the energy gap E_g are not absorbed and solar photons with $\hbar\omega > E_g$ generate electron-hole pairs which immediately lose almost all energy in excess of E_g The second intrinsic loss is due to radiative recombination. All solar cells absorb sunlight and consequently radiate light. The rate of radiative emission increases exponentially with the bias energy eV, where, for an ideal cell, V is the voltage developed across the load. The radiative current subtracts from the current delivered to the load by the cell. When V is adjusted to deliver maximum power, eV is about 0.4 to 0.5 electron volts less than E_g. This is an intrinsic loss because the radiative current of an ideal cell as a function of V is directly determined by the laws of thermodynamics and the statistical mechanical formula for the entropy of radiation.

Many papers have been written predicting the efficiencies of solar cells,[1-6] including many recent papers on multiple energy gap solar cells.[7-12] These papers try to take into account the extrinsic limitations mentioned above the thereby arrrive at maximum practical efficiencies. A different approach was taken by Muser,[13] Rose,[14] and Shockley and Queisser,[15] who considered only the limitations of thermodynamics and fundamental radiative processes in attempting to obtain the intrinsic limitations to solar-cell efficiency. Similar analyses have been carried out attempting to determine the limiting efficiencies of photochemical systems.[16,17]

Shockley and Queisser[15] calculated the efficiency of an ideal solar cell by taking into account the two intrinsic losses discussed above. They approximated the solar spectrum by a 6000-K blackbody spectrum and used the principle of detailed balance to calculate the intrinsic radiative current. The present paper is an extension of their approach. To treat the terrestrial solar cell, the blackbody spectrum is replaced by a standard air mass 1.5 terrestrial spectrum.[18] The calculations of efficiency are made by a simple graphical procedure instead of by computer calculations of numerical integrals. The graphical method has the advantage of giving a quantitative visual representation of all intrinsic losses and allowing determination of efficiencies of multiple as well as single energy gap cells.

The graphical method is presented in Sec. II and is used there to calculate the efficiencies of ideal single band-gap cells versus E_g. This calculation requires a knowledge of $E(E_g)$, the maximum work done by the cell per absorbed photon. This quantity is calculated in Sec. III. In Sec. IV, the graphical procedure is used to calculate the limiting efficiencies of 1, 2, 3, and 36 energy gap cells in concentrated sunlight. The rather impractical 36 energy gap is considered in order to determine the ultimate efficiency of a solar cell and compare it to the efficiency limit due solely to the entropy of solar radiation. This comparison is made in Sec. V, where the intrinsic thermodynamic limit to solar energy conversion is presented and the reasons why even ideal multiple energy gap cells fall below the thermodynamic limit are discussed. A brief summary is given in Sec. VI.

II. GRAPHICAL ANALYSIS OF SOLAR-CELL EFFICIENCY

The air mass 1.5 solar spectrum, recommended by the NASA/ERDA workshop on photovoltaic measurement procedures as the standard terrestrial spectrum for purposes of calculation,[18] is shown in Fig. 1 togehter with the extraterrestrial air mass 0 spectrum and a 5800-K blackbody spectrum. The dotted portion of the terrestrial spectrum for $\hbar\omega < 0.49$ eV was not supplied by the NASA/ERDA re-

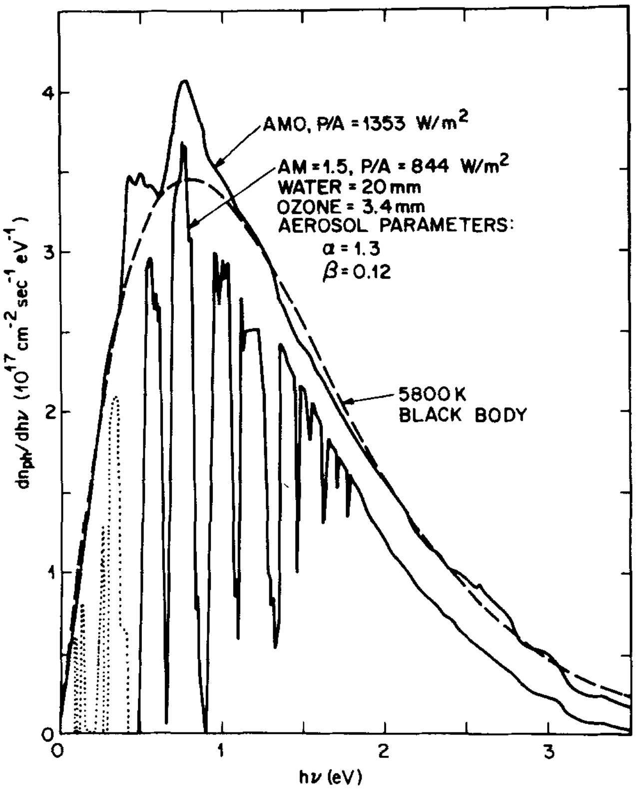

FIG. 1. A terrestrial air mass 1.5 spectrum, an extraterrestrial air mass 0 spectrum, and a 5800-K blackbody radiation spectrum. The blackbody spectrum is a reasonable fit to the air mass 0 spectrum, but not to the terrestrial spectrum which is highly structured by infrared absorption bands. The dotted portion of the terrestrial spectrum was roughly estimated from infrared absorption data.

port.[18] Instead, this portion of the spectrum was roughly estimated from the AM0 spectra and data on atmospheric infrared absorption.[19] The terrestrial solar spectrum is highly structured due to many infrared absorption bands. Consequently, numerical integrations of this spectrum, necessary in the determination of solar cell efficiencies, are tedious. A graphical procedure is described in this section for determining solar-cell efficiencies. Only a single numerical integration is necessary to implement this procedure. The integration is required to determine the function $n_{\rm ph}(E_g)$, the solar flux (in photons $\mathrm{cm}^{-2}\ \mathrm{sec}^{-1}$) absorbed by a semiconductor with energy gap E_g. The operational definition of E_g in this paper is that the semiconductor is assumed to be opaque for photon energies greater than E_g and transparent for energies less than E_g.

$$n_{\rm ph}(E_g) = \int_{E_g}^{\infty} \frac{dn_{\rm ph}}{d\hbar\omega}\, d\hbar\omega \tag{1}$$

The function $n_{\rm ph}$ is plotted versus E_g in Fig. 2.

The area under the $n_{\rm ph}(E_g)$ curve is just equal to the total solar power per unit area P/A. To see this it is convenient to regard $n_{\rm ph}$ in Fig. 2 as the independent variable and E_g to be a function $n_{\rm ph}$. Then the area under the $n_{\rm ph}$-vs-E_g curve is

$$P/A = \int_0^{N_{\rm ph}} E_g\, dn_{\rm ph} = \int_0^{\infty} E_g \frac{dn_{\rm ph}}{dE_g}\, dE_g . \tag{2}$$

The last expression is clearly equal to the solar power per unit area. If the entire solar spectrum could be converted into work, the solar-cell efficiency would be 100%. For this reason, the area of the $n_{\rm ph}(E_g)$ curves is labeled 100% in Fig. 2. The percentage of this area that is converted into work is equal to the efficiency of the solar cell.

The losses are illustrated in Fig. 2 for $E_g = 1.35$ eV, the case of highest efficiency. The three shaded areas correspond to the three intrinsic losses. The area labeled $h\nu < E_g$ is lost because photons contributing to that region are not absorbed. The area labeled $h\nu > E_g$ is lost because carriers generated by photon absorption immediately lose almost all energy in excess of E_g, when they relax to energies near the band edges. The area labeled $W < E_g$ is lost because, as discussed in Sec. I, radiative recombination limits the work done per photon W will be calculated in Sec. III. It is plotted as a function of $n_{\rm ph}$ in Fig. 2. The remaining unshaded area equals the power per unit area that the solar-cell delivers. The cell efficiency which is given by

$$\mathrm{Eff} = \frac{100 N_{\rm ph}\, W}{P/A}\,\% = \frac{100 W}{\langle h\nu \rangle}\,\% , \tag{3}$$

where $N_{\rm ph} n_{\rm ph}(0)$ and $\langle h\nu \rangle$ is the average photon energy. Both quantities are given in Fig. 2.

Inspection of Fig. 2 shows that the unshaded square goes to zero for either very large or very small values of E_g. A plot of solar-cell efficiency versus E_g is given in Fig. 3. The curve is based on a value of W valid for unconcentrated sun-

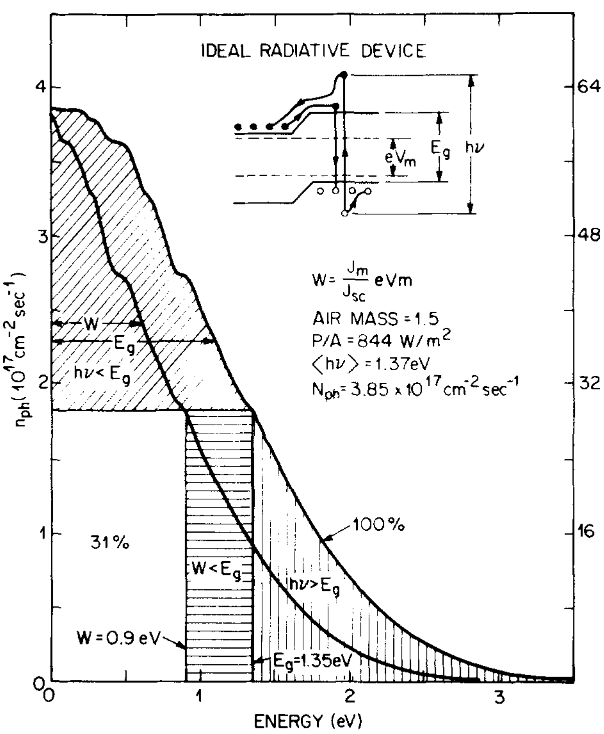

FIG. 2. Graphical analysis of the efficiency of an ideal solar cell. The outer curve is E_g versus $n_{\rm ph}$, the absorbed photon flux. The inner curve is W, the work per absorbed photon versus $n_{\rm ph}$. The area under the outer curve is the solar power per unit area. The shaded areas equal different losses as explained in the text. The unshaded area is the power per unit area delivered to the load.

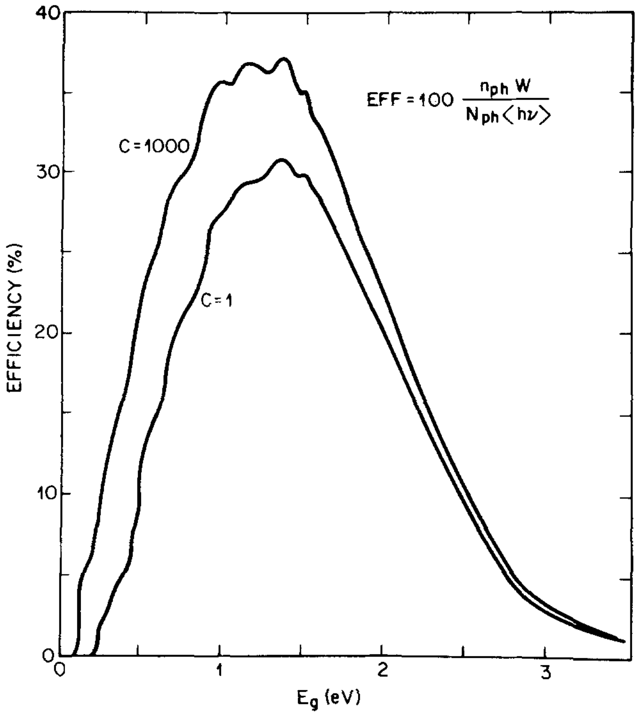

FIG. 3. Solar-cell efficiency versus energy gap for solar concentrations of 1 and 1000 suns.

light and is labeled $C = 1$ sun, where C is the solar concentration factor. We will show in Sec. III that for concentrated sunlight, W increases by $kT\ln(C)$. A curve of solar-cell efficiency versus E_g is also plotted in Fig. 3 for $C = 1000$. For both $C = 1$ and $C = 1000$, an ideal cell temperature of 300 K is assumed. The maximum efficiencies are approximately 31% at $C = 1$ and 37% at $C = 1000$.

III. CALCULATION OF THE MAXIMUM WORK DONE PER ABSORBED PHOTON

A. Rate of radiative emission

Consider the propagation of radiation across the active region of the solar cell (the region with quasi-Fermi levels of the conduction and valence bands separated by eV). Let ρ be the density of photons per unit volume, per unit angular frequency ω, and per unit solid angle Ω. Neglecting stimulated emission, ρ will be attenuated by optical absorption with coefficient α and will grow at a constant rate due to spontaneous emission. If we denote the rate of growth by spontaneous emission as $\alpha\bar{\rho}$, the equation for ρ is

$$\frac{d\rho}{dz} = -\alpha\rho + \alpha\bar{\rho}\,. \tag{4}$$

The solution of Eq. (4) is that ρ exponentially approaches a constant value $\bar{\rho}$ for large values of z. If at $z = 0$, radiation enters the active region with the density of incident thermal or solar radiation ρ_i, it will change with path length z as

$$\rho = \rho_i \exp(-\alpha z) + \bar{\rho}[1 - \exp(-\alpha z)] \tag{5}$$

We assume that for $\hbar\omega > E_g$, the cell is opaque. For these energies, the incident thermal or solar radiation will be attenuated and the light emerges from the active region with density $\bar{\rho}$.

The steady-state photon density $\bar{\rho}$ can be calculated from the laws of thermodynamics and statistical mechanics. The quasi-Fermi levels are the free energies needed to add an additional electron to the valence band or to the conduction band. When an electron drops from the conduction band to the valence band, the Helmholtz free energy released $\Delta E_s - T\Delta S_s$ is eV, the difference in quasi-Fermi levels.[20]

$$eV = \Delta E_s - T\Delta S_s\,, \tag{6}$$

where ΔE_s and ΔS_s represent the energy and entropy lost by the semiconductor.

For a system of radiation modes, equilibrium values of the energy and entropy are given by the expressions for a Bose gas[21]

$$E_r = \sum_{\omega'} \hbar\omega\,\bar{n}_{\omega'}\,, \tag{7}$$

$$S_r = k\sum_{\omega'} [(\bar{n}_{\omega'} + 1)\ln(\bar{n}_{\omega'} + 1) - \bar{n}_{\omega'}\ln(\bar{n}_{\omega'})]\,, \tag{8}$$

where the equilibrium occupation numbers $\bar{n}_{\omega'}$ are functions of $\hbar\omega'$. To find the change in energy and entropy, when an additional photon of energy $\hbar\omega$ is added to the modes, we differentiate Eqs. (7) and (8) and set $\Sigma_{\omega'}\,\Delta n_{\omega'} = 1$. (Note that only modes with $\omega' = \omega$ contribute to these changes and $\bar{n}_\omega$ is the same for each mode with angular frequency ω.) The result is that the increase in energy ΔE_r and entropy ΔS_r of the radiation modes when a photon is emitted is

$$\Delta E_r = \hbar\omega\,, \tag{9}$$

$$\Delta S_r = k\ln\left(\frac{\bar{n}_\omega + 1}{\bar{n}_\omega}\right). \tag{10}$$

We can use Eqs. (6), (9), and (10) to determine $\bar{n}_\omega$. Energy is conserved during photon emission, so $\Delta E_s = \Delta E_r$. In equilibrium, entropy does not increase during photon emission and therefore, $\Delta S_s = \Delta S_r$. Therefore, Eq. (6) becomes

$$eV = \hbar\omega - kT\ln\left(\frac{\bar{n}_\omega + 1}{\bar{n}_\omega}\right) \tag{11}$$

or

$$\bar{n}_\omega = \frac{1}{\exp[(\hbar\omega - eV)/kT] - 1} \cong \exp\left(\frac{eV - \hbar\omega}{kT}\right). \tag{12}$$

This approximation is valid because eV is many kT less than E_g. Equation (12) could have been derived from a direct calculation of the ratio of the rates of spontaneous emission and optical absorption.[22]

The radiation density $\bar{\rho}$ is found by multiplying $\bar{n}_\omega$ by the density of modes per unit volume, per unit solid angle, and per unit angular frequency given by $[2/(2\pi)^3]\,k^2(dk/d\omega)$, where $k = n\omega/c$ is the photon wave vector, $d\omega/dk = v_g$ is the group velocity, and n is the refractive index.

$$\bar{\rho} \cong \frac{1}{4\pi^2}\frac{k^2}{v_g}\exp\left(\frac{eV - \hbar\omega}{kT}\right). \tag{13}$$

Equation (13) for $\bar{\rho}$ was previously derived by Shockley and Queisser using the principle of detailed balance and by

Ross[23] with a derivation similar to this one, but beginning with Planck's law of blackbody radiation instead of Eq. (10). The corresponding values for thermal radiation are given by Eqs. (6) and (13) with $V = 0$.

The radiative current density $J_{\rm rad}$ is given by

$$J_{\rm rad} = e\int_{E_g/\hbar}^{\infty} d\omega \int d\Omega \cos(\theta)\,\bar{\rho} v_g\,. \tag{14}$$

We will assume that the active region is grown on an absorbing semiconductor substrate. (This differs from Shockley and Queisser,[15] who assume two transparent semiconductor-air interfaces.) The emitted radiation incident on the top surface of the semiconductor at angles greater than $\sin\theta = 1/n$ is totally reflected back into the active region. Consequently, the sum of contributions of both the lower and upper surfaces to the angular integral Eq. (14) is

$$\int d\Omega \cos\theta = \pi(1 + 1/n^2) \tag{15}$$

and $J_{\rm rad}$ becomes

$$J_{\rm rad} = \frac{e(n^2+1)}{4\pi^2 c^2}\int_{E_g/\hbar}^{\infty} d\Omega\, \omega^2 \exp\left(\frac{eV - \hbar\omega}{kT}\right) \cong A \exp\left(\frac{eV - E_g}{kT}\right), \tag{16}$$

where

$$A \cong \frac{e(n^2+1)\,E_g^2\,kT}{4\pi^2\hbar^3 c^2} = 5693 E_g^2\,\frac{\rm A}{\rm cm^2}\,. \tag{17}$$

E_g is in electron volts and we have estimated n as 3.6, the value for GaAs. It is clear from the above discussion that the incident absorbed thermal radiation $J_{\rm th}$ is given by $J_{\rm rad}$ with $V = 0$.

$$J_{\rm th} = A\exp(-E_g/kT)\,. \tag{18}$$

B. Calculation of the maximum work done by ideal solar cell

The current density delivered to the load is the difference of the current densities due to absorbed solar and thermal radiation and the current density of radiation emitted from the top surface or absorbed in the substrate. Defining $J_{\rm ph} = en_{\rm ph}$, we have

$$J = J_{\rm ph} + J_{\rm th} - J_{\rm rad}\,. \tag{19}$$

The second term, $J_{\rm th}$, is negligible compared to $J_{\rm ph}$ for all semiconductors with $E_g \geqslant 0.3$ eV, as can be shown by evaluation of Eq. (18). To simply the discussion we will neglect this term. Equation (19) then becomes

$$J = en_{\rm ph} - A\exp\left(\frac{eV - E_g}{kT}\right). \tag{20}$$

The open-circuit voltage is found be setting $J = 0$.

$$eV_{\rm oc} = E_g - kT\ln\left(\frac{A}{en_{\rm ph}}\right). \tag{21}$$

The maximum power point (J_m, V_m) is found by setting the derivative $d(JV)/dV = 0$. The familiar result of this calculation is

$$eV_m = eV_{\rm oc} - kT\ln\left(1 + \frac{eV_m}{kT}\right), \tag{22}$$

$$J_m = \frac{en_{\rm ph}}{1 + kT/eV_m}\,. \tag{23}$$

Finally, the work done per absorbed photon W is given by

$$W = \frac{J_m V_m}{n_{\rm ph}} = \frac{eV_m}{1 + kT/eV_m} \cong eV_m - kT\,. \tag{24}$$

Combining Eqs. (21), (22), and (24), we have

$$W \cong E_g - kT\left[\ln\left(\frac{A}{en_{\rm ph}}\right) + \ln\left(1 + \frac{eV_m}{kT}\right) + 1\right]. \tag{25}$$

Let us take GaAs as a numerical example. For this semiconductor, $E_g = 1.42$ eV and $en_{\rm ph} = 0.027$ A/cm^2. Substitution into Eq. (21) gives

$$eV_{\rm oc} = E_g - 0.334 \text{ eV} = 1.086 \text{ eV}\,.$$

Solution of Eq. (22) gives

$$eV_m = eV_{\rm oc} - 0.095 \text{ eV} = 0.991 \text{ eV}$$

and from Eq. (24) or (25) we find that the maximum work done per absorbed photon is

$$W = E_g - 0.455 \text{ eV} = 0.965 \text{ eV}\,.$$

W is plotted in Fig. 2 for different values of E_g (or $n_{\rm ph}$). The value of W is usually about 0.4 to 0.5 eV less than E_g.

For very small values of E_g, Eq. (25) indicates that W would become negative. By including $J_{\rm th}$ in Eq. (19) in the analysis, a more complicated formulas for W can be derived, which is valid at all values of E_g and which tapers smoothly

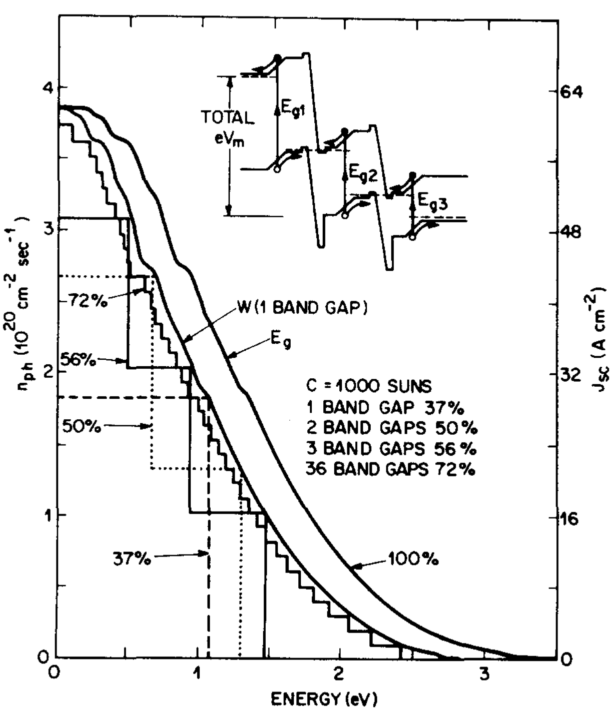

FIG. 4. Graphical analysis of the efficiencies of 1, 2, 3, and 36 energy gap solar cells. The step heights equal to the photon flux absorbed by each energy gap and the step widths (measured from the origin) equal the maximum energy per absorbed photon, delivered to the load. The efficiency of each cell is given by the ratio of the area enclosed by the steps and the area under the outer curve, labeled 100%.

to zero at small values of E_g. This was done in the calculation of W in Fig. 2.

The effect of concentrating the sunlight is given by Eqs. (21) and (25). If $n_{\rm ph}$ goes to $n_{\rm ph}C$, W increases by $kT\ln(C)$. For $kT = 0.0258$ eV and $C = 1000$, W increases by 0.18 eV.

IV. GRAPHICAL CALCULATION OF THE EFFICIENCIES OF MULTIPLE ENERGY GAP SOLAR CELLS

The efficiencies of ideal single energy gap solar cells, plotted in Fig. 3, are limited to 31% for $C = 1$ sun and 37% for $C = 1000$ suns. The low efficiency stems primarily from the inability of a single semiconductor energy gap to match the broad solar spectrum. This was discussed in Sec. I and is clearly shown by the shaded regions in Fig. 2. This situation can be improved by using several photovoltaic junctions in tandem as illustrated in the band diagram in Fig. 4, which shows three photovoltaic cells of progressively smaller energy gaps connected in series by means of tunnel junctions. Incident sunlight first encounters the highest energy gap semiconductor. The below-band-gap light is then transmitted into the second semiconductor. Finally, light with $\hbar\omega$ less than the second energy gap is transmitted into the third semiconductor.

The current flowing through a string of photovoltaic junctions connected in series will be the same for each cell. In an optimally designed device, the energy gaps would be chosen so that each photovoltaic junction delivers the same current at optimum power to the series string. This can be done by choosing the steps $\Delta n_{\rm ph}$, the rth cell from the top proportional to $(1 + kT/eV_{mr})$ [see Eq. (23)]. To simplify this procedure equal step heights $\Delta n_{\rm ph}$ were chosen. (The error in this choice is almost compensated for by the fact that the rth layer receives an additional photon flux of approximately $\cong \Delta n_{\rm ph}\, kT/eV_{m(r-1)}$ radiated from the layer above it.)

The width of the steps is W_r, the energy per absorbed photon delivered to the load by the rth semiconductor. The rth semiconductor from the top will absorb approximately only $1/r$ as many solar photons as when it is operating alone and hence its value of W will be reduced by $kT\ln(r)$ from the one energy gap case. For this reason, the corners of the steps in Fig. 4 do not quite touch the curve labeled W (one band gap).

The maximum efficiencies are found by varying $\Delta n_{\rm ph}$ until the maximum areas enclosed by the steps are found. The step heights for maximum efficiencies are shown in Fig. 4 for the case of $C = 1000$ suns and 1, 2, 3, and 36 energy gaps. The maximum efficiencies are 37, 50, 56, and 72%, respectively. The case of 1000 suns solar concentration was chosen for illustration because multiple energy gap cells are expected to be used only in concentrators having relatively high concentrations. Only then can a complex and costly cell be afforded. The impractical case of 36 energy gaps was calculated in order to try to approximately assess what the maximum efficiency is. As the number of layers increases, the efficiency of the cell will first increase as matching improves and then begin to decrease due to reductions in W caused by the $kT\ln(r)$ correction. No attempt was made to find the number of energy gaps giving the exact maximum efficiency.

V. THERMODYNAMIC LIMITS TO ENERGY CONVERSION

In Sec. IV, we found that an ideal 36 energy gap solar cell, operating at a concentration of 1000 suns, would have an efficiency of about 72%. This efficiency is large, but it is still well below the thermodynamic limit for converting the energy of solar radiation into work. In this section, we will establish the thermodynamic limit and then discuss in detail why the efficiency of the ideal photovoltaic energy converter falls below this limit.

Consider a quantity of sunlight of energy E and entropy S which is transformed by an ideal solar energy converter into work W and heat Q. The heat is assumed to pass into the surroundings at temperature $T = 300$ K. Assume that these changes take place with no net increase in entropy. Then, from the first and second laws of thermodynamics, we have

$$E = W + Q, \tag{26}$$

$$Q = TS. \tag{27}$$

Therefore, the maximum efficiency of conversion, $100W/E$, is

$$\mathrm{Eff}_{\max} = 100(1 - TS/E). \tag{28}$$

The expressions for the energy and entropy of solar radiation can be calculated from Eqs. (7) and (8). Figure 1 shows that the solar radiation spectrum can be approximated by blackbody spectrum at temperature $T_s \approx 5800$ K. For such a spectrum it is well known that

$$S = \tfrac{4}{3} E/T_s. \tag{29}$$

Therefore, the maximum efficiency of solar energy conversion is given by Eq. (28) as

$$\mathrm{Eff}_{\max} = 100(1 - \tfrac{4}{3} T/T_s) = 93\%. \tag{30}$$

This efficiency was previously found by Press,[24] who calculated the work derived from an adiabatic expansion of a volume of solar radiation.

The maximum solar efficieincy is slightly less than that of a Carnot engine run between temperatures of T_s and T. That efficiency would be

$$\mathrm{Eff}_{\rm Carnot} = 100(1 - T/T_s) = 95\%. \tag{31}$$

The discrepancy is due to the fact that the emission of radiation from the sun is an irreversible process. In a Carnot radiation engine, the radiation would be emitted into a slowly expanding cylinder. Then, the input energy is greater by PV and equal to $E + PV = \tfrac{4}{3}E$, while the heat exhausted is the same. Consequently, Eqs. (26), (27), and (29) can be combined to give Eq. (31), the Carnot efficiency.

The ideal multiple energy gap solar cell falls short of the performance of an ideal solar energy converter because entropy increases in several ways. First, each junction of the solar cell emits radiation in all directions, not just within the angular aperture of the incident radiation. Second, the radiated energy is lost. To diminish this loss and maximize energy conversion, the cell is operated irreversibly at the maximum power point, where entropy increases during the conversion of sunlight into work and heat. For these reasons, the efficiency of the ideal multiple energy gap solar solar cell is 72% instead of the thermodynamic limit of 93%. We will now discuss the contributions to the differences in the two efficiencies in more detail.

The increase in entropy associated with reemission of radiation into more modes than originally occupied by the incident sunlight can be avoided in principle. For example, instead of an arrangement of stacked junctions, beam splitters could be used to direct the different components of sunlight onto different cells. If these cells are made of transparent substrates with perfectly reflecting backs, the number of modes of radiation leaving each cell would be reduced by $1 + n^2$, where $n \simeq 3.6$ is the refractive index of the cell. The operating voltage cell would then increase by $kT \ln(1 + n^2)$, resulting in an increase in efficiency of

$$\frac{100kT \ln(1 + n^2)}{\langle h\nu \rangle} \cong 5\% , \tag{32}$$

where $\langle h\nu \rangle = 1.37$ eV.

The ratio of the number of modes radiating from each photovoltaic junction to the number of incident modes absorbed by each junction is

$$\frac{\pi kT}{C\Omega_s \Delta E_g},$$

where $\Omega_s = 6.8 \times 10^{-5}$ steradians is the solid angle subtended by the sun, ΔE_g is the difference in energy gaps between semiconductors, and C is the solar concentration. The optimum energy gap separation is $\Delta E_g \approx kT$. For larger separations, energy is lost when the carriers relax to within $\approx kT$ of the band edges. If this energy gap separation is used, the ratio of emission modes to absorption modes can be made equal to unity by increasing C to the maximum concentration C' given by

$$C' = \frac{\pi}{\Omega_s} = 46\,200 . \tag{33}$$

At this concentration, light impinges on the top surface of the cell from all directions. The increase in operating voltage due to the increase in concentration is $kT \ln(C'/C)$ and the efficiency increases by

$$\frac{100kT \ln(C'/C)}{\langle h\nu \rangle} \cong 7\% . \tag{34}$$

The remaining discrepancy between the ideal multiple energy gap photovoltaic energy converter and the ideal solar energy converter is due to the reemission of light from the cell. This energy is lost, whereas in a heat engine, energy radiated back to the heat source is not counted as a loss. To maximize solar energy conversion, cells are operated at the maximum power point. We showed in Sec. III, Eq. (22), that this costs a work per converted photon of $eV_{oc} - eV_m = kT \ln(1 + eV_m/kT)$. If we roughly estimate the average value of eV_m as 84% of $\langle h\nu \rangle$ or 1.15 eV, this loss in efficiency is

$$\frac{100kT \ln(1 + \langle eV_m \rangle/kT)}{\langle h\nu \rangle} \cong 7\% . \tag{35}$$

At the maximum operating point, according to Eq. (24), the work per incident photon lost by radiation from the cell is kT. This results in a loss in efficiency of about

$$\frac{100kT}{\langle h\nu \rangle} \cong 2\% . \tag{36}$$

The sum of efficiency losses given by Eqs. (32) and (34)–(36) is 21%, which when added to the ideal photovoltaic efficiency of $\approx 72\%$ gives 93%, exactly the thermodynamic limit. This exact accounting is probably fortuitous since the various approximations used and the uncertainties in the 72% figure have probably introduced errors of 1 or 2%.

VI. SUMMARY

An analysis has been made of the efficiencies of ideal solar cells that are opaque above an energy E_g and have no nonradiative recombination or other extrinsic limitations. The intrinsic limitations to solar-cell efficiency were reviewed in Sec. I. They are the same as previously discussed by Shockley and Queisser.[15] This paper extends the approach of Shockley and Queisser[15] in the following ways:

(1) a graphical analysis is made that clearly shows the magnitudes of the losses;

(2) multiple as well as single energy gap cells are considered;

(3) a terrestrial solar spectrum is used;

(4) the effect of concentrated sunlight is considered;

(5) the thermodynamic limit to solar energy conversion is discussed and the reasons why ideal solar-cell efficiencies fall below this limit are discussed.

The *J-V* relation for an ideal solar cell is derived in a manner similar to that given by Ross.[23] It is shown that this *J-V* relation is determined by the laws of thermodynamics and statistical mechanics.

The maximum efficiencies of ideal solar cells were found to be 31% at 1 sun intensity. At 1000 suns concentration and with the solar cell held at room temperature, ideal 1, 2, 3, and 36 energy gap cells have efficiencies of 37, 50, 56, and 72%, respectively. The 72% efficiency represents the efficiency of an ideal solar cell that is almost perfectly matched to the entire solar spectrum. It is less than the thermodynamic limit of 93% because energy is lost and entropy increases when light is emitted from the *p-n* junctions in all directions. The solar cell must operate away from equilibrium ($eV_m < eV_{oc}$) in order to minimize light emission.

ACKNOWLEDGMENTS

The author has benefitted from discussions with H. Ehrenreich, J.J. Hopfield, R.S. Knox, R.C. Miller, A. Rose, and E. Yablonovitch.

[1]M. B. Prince, J. Appl. Phys. **26**, 534 (1955).

[2]J. J. Loferski, J. Appl. Phys. **27**, 777 (1956).

[3]J. J. Wysocki and P. Rappaport, J. Appl. Phys. **31**, 571 (1960).

[4]M. Wolf, Proc. IRE **48**, 1246 (1960).

[5]J. A. Fossum, E. L. Burgess, and F. A. Lindholm, Solid State Electron. **21**, 729 (1979).

[6]H. J. Hovel, *Semiconductor and Semimetals*, edited by R. K. Willardson and A. C. Beer (Academic, New York, 1975), Vol. 11.

[7]R. L. Moon, L. W. James, H. A. VanderPlas, T. O. Yep, G. A. Antypas, and Y. Chai, 13th IEEE Photovoltaic Specialists Conference, 1978, p. 859 (unpublished).

[8]G. M. Masden and C. E. Backers, Ref. 7, p. 853.

[9]A. Bennet and L. C. Olsen, Ref. 9, p. 868.
[10]L. M. Fraas and R. C. Knechtli, Ref. 7, p. 886.
[11]J. A. Cope, J. S. Harris, Jr., and R. Sahai, Ref. 7, p. 881.
[12]M. F. Lamorte and D. Abbot, Ref. 7, p. 874.
[13]H. A. Muser, Z. Phys. **148**, 380 (1957).
[14]A. Rose, J. Appl. Phys. **31**, 1640 (+960).
[15]W. Shockley and H. A. Queisser, J. Appl. Phys. **32**, 510 (1961).
[16]R . T. Ross and Ta-Lee Hsiao, J. Appl. Phys. **48**, 4783 (1977).
[17]Work in this field has been recently reviewed by R. S. Knox, [Proceedings of the Dahlim Workshop on Light-induced Charge Separation at Interfaces in Biological and Chemical Systems, Berlin, 1978 (unpublished).
[18]ERDA/NASA Report 1022-77/16 on terrestrial photovoltaic measurement procedures.
[19]D. M. Gates and W. J. Harrop, Appl. Opt. **2**, 887 (1963).
[20]W. Shockley, *Electrons and Holes in Semiconductors* (Van Nostrand, New York, 1950), p. 464.
[21]L. D. Landau and E. M. Lifshitz, *Statistical Physics*, 2nd ed. (Addison-Wesley, Reading, Mass., 1970), Sec. 54 on the nonequilibrium Bose gas.
[22]H. Bebb and E. W. Williams, in *Semiconductors and Semimetals*, edited by R. K. Willardson and A. C. Beer (Academic, New York, 1972), Vol. 8, p. 206.
[23]R. T. Ross, J. Chem. Phys. **46**, 4590 (1967).
[24]W. H. Press, Nature **264**, 735 (1976).